

A&A manuscript no.
(will be inserted by hand later)

Your thesaurus codes are:

1 (11.09.1 LRG J0239–0134 ; 11.05.2; 11.09.2; 11.19.1; 12.03.3; 12.07.1)

ASTRONOMY
AND
ASTROPHYSICS

A ring galaxy at $z = 1$ lensed by the cluster Abell 370 *

G. Soucail¹, J.P. Kneib¹, J. Bézecourt^{1,2}, L. Metcalfe³, B. Altieri³, and J.F. Le Borgne¹

¹ Observatoire Midi-Pyrénées, Laboratoire d'Astrophysique, UMR 5572, 14 Avenue E. Belin, F-31400 Toulouse, France

² Kapteyn Institute, Postbus 800, 9700 AV Groningen, The Netherlands

³ ISO Data Centre, Astrophysics Division, Space Science Department of ESA, Villafranca del Castillo, PO Box 50727, E-28080 Madrid, Spain

Received soon , Accepted immediately

Abstract. We present a study of a very peculiar object found in the field of the cluster-lens Abell 370. This object displays, in HST imaging, a spectacular morphology comparable to nearby ring-galaxies. From spectroscopic observations at the CFHT, we measured a redshift of $z = 1.062$ based on the identification of [O II] 3727 Å and [Ne V] 3426 Å emission lines. These emission lines are typical of starburst galaxies hosting a central active nucleus and are in good agreement with the assumption that this object is a ring-galaxy. This object is also detected with ISO in the LW2 and LW3 filters, and the mid Infra-Red (MIR) flux ratio favors a Seyfert 1 type. The shape of the ring is gravitationally distorted by the cluster-lens, and most particularly by a nearby cluster elliptical galaxy. Using the cluster mass model, we can compute its intrinsic shape. Requiring that the outer ring follows an ellipse we put constraints on the M/L ratio of the nearby galaxy and derive the magnification factor. The luminosities of the source at various wavelengths are then discussed.

Key words: Galaxies: individual: LRG J0239–0134 – Galaxies: evolution – Galaxies: interactions – Galaxies: Seyfert – Cosmology: observations – gravitational lensing

1. Introduction

A useful property of gravitational lensing is the magnification of light: the gain in spatial resolution allows the morphological properties of distant and resolved objects to be probed in greater detail and the gain in apparent flux allows fainter sources that would otherwise neither be detected nor studied to be probed statistically. Massive clusters of galaxies are ideal lenses for which to take

advantage of these magnification properties over a reasonable field of view of several square arcminutes, allowing study of a fair number of distant sources. Cluster-lenses can then be used as natural “gravitational telescopes” to address several astrophysical problems related to the properties and nature of high redshift galaxies. Morphological properties of distant lensed sources were first addressed by Smail et al. (1996) who estimated the intrinsic linear sizes of the galaxies and showed them to be compatible with a significant size evolution with redshift. Recently, a number of high- z arcs and arclets have been confirmed spectroscopically (*e.g.* Mellier et al. 1991, Ebbels et al. 1996, Trager et al. 1997, Frye & Broadhurst 1998). A detailed analysis of their intrinsic size and morphology is then possible using lens modeling. Most of them appear to be knotty with a more complex morphology than their local counterparts (Colley et al. 1996, Franx et al. 1997, Pelló et al. 1999).

In this letter, we study a peculiar object detected in the field of the galaxy cluster A370. On the HST/WFPC2 images, it displays an unusual morphology similar to nearby ring-galaxies but gravitationally distorted by the cluster. Section 2 summarises the various observations related to this source: HST imaging, spectroscopic and photometric data including mid-IR photometry obtained with ESA’s ISO spacecraft (Kessler et al. 1996). Section 3 discusses the spectral energy distribution (SED) of the object. The source reconstruction of the ring and a morphological analysis is presented in Section 4, and discussion and conclusions are presented in the last section. Throughout the paper, we consider a Hubble constant of $H_0 = 50 \text{ km s}^{-1} \text{ Mpc}^{-1}$, with $\Lambda = 0$ and $\Omega = 1$.

2. Observations

2.1. HST imaging

In the deep F675W HST/WFPC2 image described in detail in Bézecourt et al. (1999a, hereafter Paper I), a spectacular distorted ring is detected close to a bright cluster elliptical (#32 in the numbering scheme of Mellier et al. (1988) with $z = 0.370$). The object displays a clearly

Send offprint requests to: G. Soucail, soucail@obs-mip.fr

* Based on observations with the NASA/ESA *Hubble Space Telescope* obtained from the data archive at the Space Telescope European Coordinating Facility, with ISO, an ESA project with instruments funded by ESA Member States with the participation of ISAS and NASA, and with the Canada-France-Hawaii Telescope at Mauna Kea, Hawaii, USA.

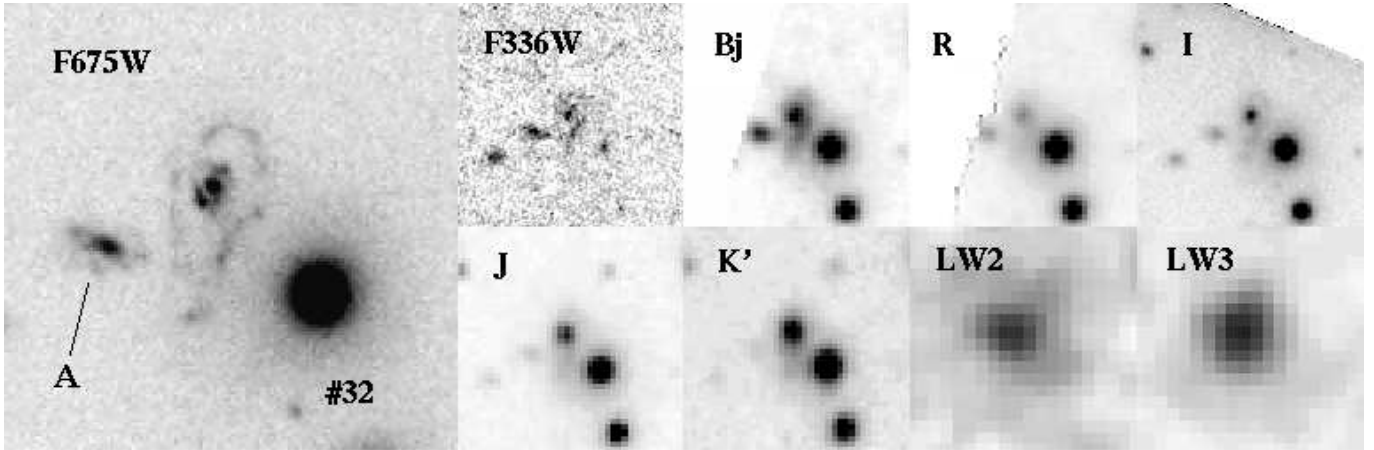


Fig. 1. Multi-colour images of the ring galaxy and its surroundings. The enlarged one comes from the HST F675W image (with a $12''$ size) while the others are multi-wavelength images ($20''$ size) of the field, from U (F336W) to mid-IR ($15\ \mu\text{m}$). See text for more details about the photometry.

resolved central bulge surrounded by a $4.8''$ -diameter distorted ring and probably a secondary $1.5''$ -diameter inner ring (Figure 1). This object is very similar in aspect to the Cartwheel galaxy (Struck et al. 1996), although the outer ring is clearly gravitationally distorted by the cluster. We used the APM catalogue to measure the astrometry of the field. The absolute coordinates of the lensed ring galaxy are: $\alpha_{J2000} = 2\text{h } 39\text{m } 56.51\text{s}$, $\delta_{J2000} = -1^\circ 34' 25.66''$ (with a $0.2''$ rms accuracy). Therefore we reference hereafter this object as: LRG J0239–0134.

A photometric analysis was performed on the F675W HST image. First, the nearby galaxy # 32 was subtracted after a radial fit of the isophotes with the “ELLIPSE” package in the IRAF/STSDAS environment. The total integrated flux for LRG J0239–0134 gives a magnitude $R_{675W} = 20.73 \pm 0.1$ that can be separated into the outer ring contribution $R_{675W} = 21.4 \pm 0.2$ and the emission of the central part $R_{675W} = 21.51 \pm 0.02$. In the HST/WFPC2 U-Band image (see Bézecourt et al. 1999b) the ring-like object is also detected and appears less centrally concentrated than in F675W. However the lower signal-to-noise prevents a detailed morphological analysis of the extended emission (Figure 1).

2.2. Spectroscopic and photometric observations

Spectroscopic data were obtained during a CFHT run using the OSIS-V instrument (Le Fèvre et al. 1994) in August 1997. A $1''$ -wide long-slit was positioned through the central bulge and the ring, with no strong contamination by the envelope of galaxy #32. We used the 2Kx2K Loral thinned CCD and the grism R150 which gives a dispersion of $6\ \text{\AA}/\text{pixel}$, with a resolution of $18\ \text{\AA}$ within the wavelength range 5000 to 9000 \AA . Two 1.8 ksec exposures were obtained just before morning twilight. The first exposure is of lower quality because of the stronger sky contribu-

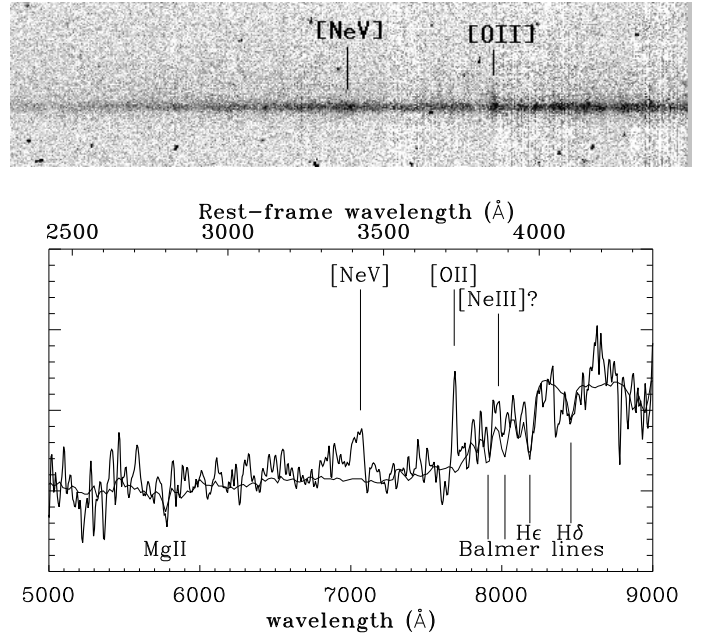


Fig. 2. Spectrum of the ring galaxy superimposed on a synthetic spectrum of a late-type spiral redshifted to $z = 1.062$. The most prominent lines are identified. Above is the original 2D spectrum after sky subtraction, showing in particular the spatial extent of the emission line at 7685 \AA .

tion. The data were reduced with standard procedures for flat-fielding, wavelength and flux calibration. Sky subtraction was performed on the 2D image (Figure 2). Several features are detected: a strong emission line at $\lambda = 7685\ \text{\AA}$, a weaker one at $\lambda = 7064\ \text{\AA}$ and an absorption line at $\lambda = 5773\ \text{\AA}$, all visible on the 2D spectrum. We unambiguously identify those lines as: [O II] 3727 \AA , [Ne V] 3426 \AA and Mg II 2800 \AA giving a redshift of $z = 1.062$

Table 1. Multi-wavelength fluxes of the ring galaxy (see text for more details). These fluxes are not corrected for the gravitational magnification of the source.

Filter	λ (μm)	Magnitude	Flux (μJy)
U _{336W}	0.336	21.00 ± 0.2	4.45
B _j	0.450	21.81 ± 0.2	6.36
R	0.646	20.38 ± 0.4	21.3
R _{675W}	0.673	20.66 ± 0.1	15.8
I	0.813	19.31 ± 0.2	45
J	1.237	17.82 ± 0.2	118
K'	2.103	16.34 ± 0.2	212
LW2	6.7		750
LW3	14.3		1800

for the source. Moreover, a tentative identification at this redshift may suggest weak emission from the [Ne III] 3869 Å line though the spectrum is contaminated by sky residuals. The [O II] line is more spatially extended than the underlying stellar continuum, and a contribution from the ring itself is likely, which is not the case for the [Ne III] line. Furthermore, the fit of the continuum with a typical late-type spiral galaxy is satisfactory and confirms the location of several Balmer absorption lines (*e.g.* H δ , H ϵ). Redder lines fall outside the visible range and unluckily, H α lies at 1.353 μm , a wavelength domain hardly detectable from the ground (outside the J-band).

Multi-band photometry of this galaxy is available from a large set of data existing on the cluster Abell 370. In addition to the HST U and R images, we used B, R and I magnitudes from deep CFHT images (Kneib et al. 1994). Near IR data were obtained with the Redeye camera at CFHT in August 1994. The final near-IR images correspond to deep exposures with integration times as long as 3.4 ksec in J and 7.2 ksec in K' in good observing conditions. The details of this photometric setup will be published elsewhere. The photometry of the ring galaxy is summarised in Table 1 with the corresponding images displayed in Figure 1. From this multi-band photometry, a photometric redshift of 0.95 ± 0.1 was found (R. Pelló, private communication) confirming the spectroscopic identification through the fit of the continuum and its stellar contribution. In addition, the fainter object close to the ring (labelled A in Figure 1) has a photometric redshift $z_{\text{phot}} = 0.4 \pm 0.1$ and is therefore not related to the ring-galaxy.

2.3. ISO data

The ring galaxy was detected with the ISO camera (ISOCAM, Césarsky et al., 1996), as part of a programme of imaging through gravitational lensing clusters (Metcalf et al. 1999). A370 was deeply imaged on a wide $7' \times 7'$ field, in micro-scanning mode, with the $3''$ pixel-field-of-view,

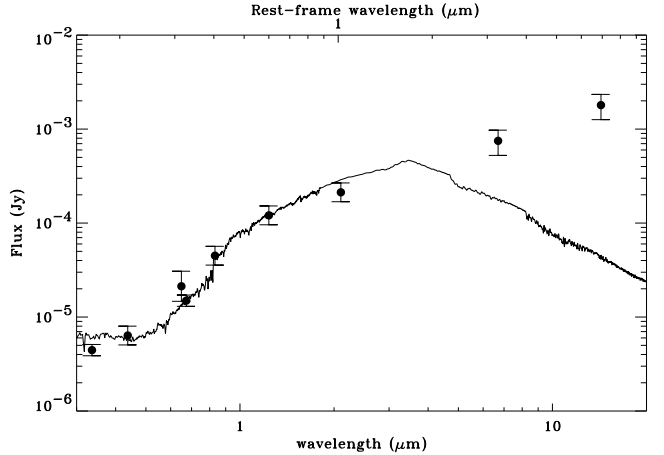


Fig. 3. Spectral Energy distribution of the ring galaxy. The data correspond to the observed photometry from 0.3 μm to 15 μm . The curve corresponds to the synthetic SED of an Sc galaxy from Fioc and Rocca-Volmerange (1996). The mid-IR excess is clearly non-stellar.

and using two broad-band, high-sensitivity filters: LW2 (5–8.5 μm) and LW3 (12–18 μm) with a total exposure time of 16.1 ksec in the deepest part of the image. The data were reduced following two substantially independent methods: a Multi-resolution Median Transform method (PRETI, Starck et al. 1998), and the Vilsa method described in Altieri et al. (1998). The photometric accuracy achievable for such faint mid-IR sources, allowing for all uncertainties in the data reduction, is around 30%. In both ISO bandpasses, the ring-galaxy is the brightest extragalactic source in the field covered by ISOCAM, apart from the giant arc. With an absolute astrometric accuracy of about $1''$ for ISOCAM after drizzling, the correspondance between the ring-galaxy and the ISO source is quite secure.

3. Spectral Energy Distribution of the galaxy

Joining together all the multi-wavelength photometric measurements, we can construct the spectral energy distribution (SED) of the galaxy over a large wavelength range (Fig. 3). This range covers both the rest-frame stellar emission and the IR flux emitted by the warm component of the ISM. The significant excess of light emitted in the mid-IR with respect to the stellar contribution can originate from three possibilities: either a central active nucleus heats the dust torus around it or warm dust is heated by a violent starburst induced by the merger that produced the ring, or we are witnessing a combination of the two phenomena. A strong argument in favour of an active nucleus is the detection of the [Ne V] emission line in the optical spectrum which is typical of Seyfert galaxies. Moreover, the rest of the optical emitted light is clearly stellar, with Balmer absorption lines and a typical stellar continuum. This suggests that a starburst is occurring and

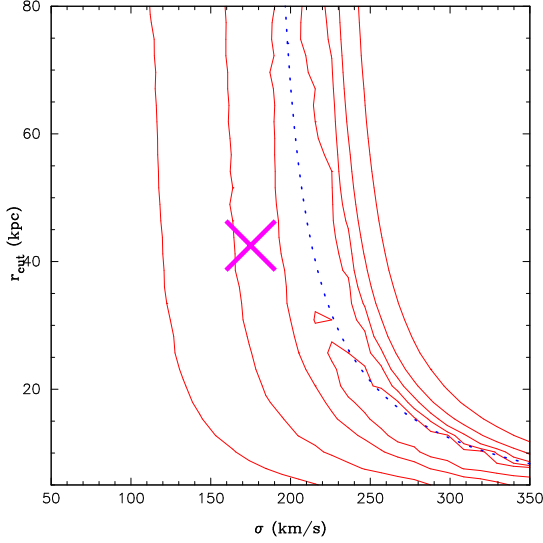


Fig. 4. Iso-contour plot of the estimator E for the galaxy #32 when fitting the outer ring to be projected as an ellipse in the source plane. The dotted line corresponds to models with iso mass within the aperture a_{32} (see text for more details).

may dominate the optical light. For this target in the mid-IR it is difficult to discriminate the contribution due to the nuclear emission from the starburst contribution, as in the case of the Cartwheel galaxy (Charmandaris et al. 1998). The flux ratio LW3/LW2 is about 2.4 (or equivalently the spectral index is about -1.15) while it is 1.1 in the nucleus and 3.8 for the ring in the Cartwheel. Taking into account the fact that we observe the rest-frame fluxes at $3.3 \mu\text{m}$ and $7 \mu\text{m}$, this can be compared easily with the mid-IR spectra shown by Schultz et al. (1998) for different types of AGN. Our results clearly favour a Seyfert 1 type, in accordance with the weak detection of the [Ne v] emission line in the optical spectrum.

4. Source Reconstruction of the lensed ring galaxy

This ring-galaxy is magnified and distorted by the gravitational shear induced by the cluster and the nearby elliptical cluster galaxy #32. This is particularly visible in the distorted shape of the outer ring. In order to reconstruct its true intrinsic size and shape we traced the rays back through the lens into the source plane, using the model proposed in Paper I. This model was optimised from the identification of several multiple images detected on the HST images and takes into account the mass halos of the brightest galaxies using standard scaling laws (Kneib et al. 1996, Natarajan et al 1998, Hjorth & Kneib 1999) related to their luminosities and depending on the properties of the

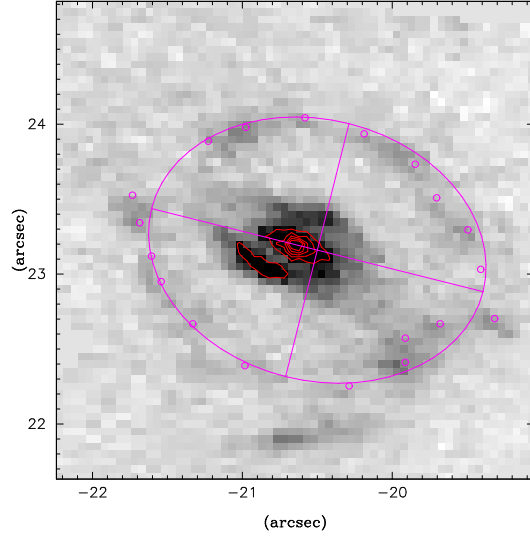


Fig. 5. Image-reconstruction of the ring galaxy in the source plane for the best fit parameters. The bottom part of the ring was not included in the fitting. This reconstruction suggests that this object does not belong to the outer ring.

Fundamental Plane:

$$\sigma_0 = \sigma_{0*} \left(\frac{L}{L_*} \right)^{\frac{1}{4}}, \quad r_t = r_{t*} \left(\frac{L}{L_*} \right)^{0.8}, \quad r_0 = r_{0*} \left(\frac{L}{L_*} \right)^{\frac{1}{2}}.$$

In particular for the elliptical galaxy #32 ($R_{675W} = 18.47$) this means that $L_R = 2.17 \cdot 10^{11} h_{50}^{-2} L_{\odot}$ which translates to $\sigma_0 = 173 \text{ km/s}$, $r_t = 42.4 h_{50}^{-1} \text{ kpc}$ (or $6.8''$ at the cluster redshift) and a total M/L ratio of $6.35 h_{50} (M/L)_{\odot}$ for this galaxy and its halo. Within the aperture $a_{32} = 26.76 h_{50}^{-1} \text{ kpc}$ defined by the distance from #32 to the ring galaxy nucleus we have $M(< a_{32})/L = 52.8 h_{50} (M/L)_{\odot}$.

We then examined the influence of the parameters (σ_0, r_t) in the source reconstruction. In order to quantify this we identified in the image plane 20 points (x_i, y_i) describing the outer ring. We then tuned the two parameters (σ_0, r_t) to check how close to an ellipse the corresponding source points (x_{si}, y_{si}) are. For this purpose we defined the following estimator:

$$E(\sigma_0, r_t) = \frac{1}{N} \sum_{i=1}^N |f_{\sigma_0, r_t}(i)|$$

with

$$f_{\sigma_0, r_t}(i) = \frac{[(x_{si} - x_c) \cos \theta - (y_{si} - y_c) \cos \theta]^2}{a^2} + \frac{[(x_{si} - x_c) \sin \theta + (y_{si} - y_c) \sin \theta]^2}{b^2} - 1$$

where (x_c, y_c, a, b, θ) are the parameters of the ellipse that minimise, for each set of (σ_0, r_t) , the estimator E. For a set of points belonging to an ellipse, E is zero. Furthermore, by definition, E is scale-invariant and does not depend on

the intrinsic size of the ring, which is one of the results of the fit. Figure 4 shows iso-contours of the estimator $E(\sigma_0, r_t)$. The original point of the model of paper I is indicated as a cross. There is clearly a degeneracy in the models that follows a constant M/L ratio within the aperture a_{32} . Fixing $r_t = 42.5 h_{50}^{-1} \text{ kpc}$, the best value for the velocity dispersion is $\sigma_0 = 220 \text{ km/s}$, which corresponds to a correction factor of 1.4 for the aperture mass leading to $M(< a_{32})/L = 4.0 (M/L)_\odot$.

The magnification factor of the source has a mean value of 2.5 but ranges from 3.6 to 2.1 depending on the distance to galaxy #32 (Figure 5). The intrinsic radius for the outer ring found is $7.7 \pm 0.4 h_{50}^{-1} \text{ kpc}$, a value comparable with the characteristics of nearby similar objects and the B-absolute luminosity of the source, corrected from the magnification and measured directly from the I magnitude is $F_B = 1.3 \cdot 10^{12} L_\odot$, about 10 times brighter than the Cartwheel galaxy (Appleton & Marston 1997).

5. Discussion

Summarising all the available data presented in this paper, we can analyse in detail the nature of the source: first, the outer ring of the galaxy constitutes good evidence for a starburst induced by a recent gravitational interaction, although the progenitor is not yet identified. The presence of an extended [O II] 3727 Å emission line in the 2D spectrum demonstrates the occurrence of star formation in the ring. In addition, the galaxy hosts an active nucleus in the centre, probably powered by the interaction and confirmed both by the detection of the [Ne v] line in the optical and by the properties of the mid-IR fluxes. This source also corresponds to the source labelled L3 by Smail et al. (1998) and detected in the sub-millimeter domain with SCUBA. This means that a cold dust emission arises from the source, but without adequate spatial information no conclusion can be drawn about the preferred location of this cold dust (ring or nucleus). We can also compute its intrinsic mid-IR luminosity, after correction for both the gravitational magnification and a k-correction estimated from a power-law fit of the spectrum. This gives $F(3.3\mu\text{m}) = 1.7 \cdot 10^{23} \text{ W/Hz}$ and $F(7\mu\text{m}) = 3.7 \cdot 10^{23} \text{ W/Hz}$, or equivalently in solar luminosity: $\nu L_\nu \simeq 4 \cdot 10^{10} L_\odot$. If we compare these values to the other SCUBA source identified in Abell 370 at $z = 2.8$ (Ivison et al. 1998) it is fainter by a factor 4 only and remains intrinsically one of the brightest mid-IR sources in the field.

To get a better understanding of the physical processes occurring in LRG J0239-0134 and to disentangle the contribution of the AGN from a starburst induced by a gravitational collision, higher resolution images at various wavelengths are clearly needed. Millimeter and sub-mm imaging may be obtained with the IRAM interferometer or in the future with the LSA/MMA while mid-IR and H α imaging must wait for the NGST. Anyhow this kind

of object represents evidence for an increase in the number of galaxy interactions at high redshift and highlights the consequences for the star formation activity in these relatively young objects.

Acknowledgements. We wish to thank Roser Pelló for her help in the estimations of photometric redshifts of the objects and Danièle Alloin for fruitful discussions about AGN optical spectra. Many thanks to Ian Smail, Rob Ivison, Andrew Blain and Jim Higdon for useful discussions. This research has been partly conducted under the auspices of a European TMR network programme made possible via generous financial support from the European Commission (<http://www.ast.cam.ac.uk/IoA/lensnet/>).

References

- Appleton P.N. & Marston A.P., 1997, AJ 113, 201
- Altieri B., Metcalfe L., Ott S. et al., 1998, "ISOCAM Faint Source report" (<http://www.iso.vilspa.esa.es>)
- Bézecourt J., Kneib J.P., Soucail G., Ebbels, T.M.D., 1998b, A&A, in press (astro-ph/9810199, Paper I)
- Bézecourt J., Soucail G., Ellis R.S., Kneib J.P., 1999, in preparation (paper II)
- Césarsky C.J. et al., 1996, A&A 315, L32
- Charmandaris V., et al., 1998, A&A, in press (astro-ph/9810276)
- Colley W.N., Tyson J.A., Turner E.L., 1996, ApJ 461, L83
- Ebbels T.M.D., Le Borgne J.F., Pelló R., Kneib J.-P., Smail I.R., Sanahuja B., 1996, MNRAS 281, L75
- Fioc M., Rocca-Volmerange B., 1996, A&A 326, 950
- Franx M., Illingworth G.D., Kelson D.D., van Dokkum P.G., Tran K-V., 1997, ApJ 486, L75
- Frye B., Broadhurst T., 1998, ApJ, 449, L115
- Hjorth, J., Kneib, J.-P., 1999, ApJ, submitted.
- Ivison R.J., Smail I., Le Borgne J.F., Blain A.W., Kneib J.P., Bézecourt J., Kerr T.H., Davies J.K., 1998, MNRAS 298, 583
- Kessler et al., 1996, A&A 315, 27
- Kneib J.-P., Mathez G., Fort B., Mellier Y., Soucail G., Longaretti P.-Y., 1994, A&A, 286, 701
- Kneib J.-P., Ellis R.S., Smail I., Couch W.J., Sharples R.M., 1996, ApJ, 471, 643
- Le Fèvre O., Crampton D., Felenbok P., Monnet G., 1994, A&A, 282, 325
- Natarajan, P., Kneib, J.-P., Smail, I.R., Ellis, R.S 1998, ApJ, 499, 600
- Mellier Y., Soucail G., Fort B., Mathez G., 1988, A&A, 199, 13
- Mellier Y., Fort B., Soucail G., Mathez G., Cailloux M., 1991, ApJ, 380, 334
- Metcalfe L., Altieri B., McBreen, B. et al., 1999 To appear in ESA conference Proceedings of the "The Universe as seen by ISO", October 1998, Unesco, Paris, France.
- Pelló R., et al., 1999, submitted, astro-ph/9810390
- Smail I., Dressler A., Kneib J.P., Ellis R.S., Couch W.J., Sharples R.M., Oemler A.Jr, 1996, ApJ 469, 508
- Smail I., Ivison R.J., Blain A.W., Kneib J.P., 1998, ApJ 507, L21
- Starck J. L. et al., 1998, in *Extragalactic Astronomy in the Infrared*, Editions Frontières, G. Mamon Ed.

- Schultz et al. Schultz B., Clavel J., Altieri B. et al., 1999 To appear in ESA conference Proceedings of the "The Universe as seen by ISO", October 1998, Unesco, Paris, France.
- Struck C., Appleton P.N., Borne K.D., Lucas R.A., 1996, AJ 112, 1868
- Trager S.C., Faber S.M., Dressler A., Oemler A., 1997, ApJ, 485, 92